Defect formation preempts dynamical symmetry breaking in closed quantum systems

Carmine Ortix,[1] Jorrit Rijnbeek,[2] and Jeroen van den Brink[1]

[1]*Institute for Theoretical Solid State Physics, IFW Dresden, D-01171 Dresden, Germany*
[2]*Institute-Lorentz for Theoretical Physics, Universiteit Leiden, NL-2300 RA Leiden, The Netherlands*

The theory of spontaneous symmetry breaking—one of the cornerstones of modern condensed-matter physics—underlies the connection between a classically ordered object in the thermodynamic limit and its microscopic quantum-mechanical constituents. However, a large, but not infinitely large, system requires a finite symmetry-breaking perturbation to stabilize a symmetry-broken state over the exact quantum-mechanical ground state, respecting the symmetry. Here, we use the example of a particular antiferromagnetic model system to show that no matter how slowly such a symmetry-breaking perturbation is driven, the adiabatic limit can never be reached. Dynamically induced collective excitations—"quantum defects"—preempt the symmetry-breaking phenomenon and trigger the appearance of a symmetric nonequilibrium state that recursively collapses into the classical equilibrium state, breaking the symmetry at punctured times. The presence of this state allows "quantum-classical" transitions to be investigated and controlled in mesoscopic devices by externally supplying a proper dynamical symmetry-breaking perturbation.

I. INTRODUCTION

The relation between quantum physics at microscopic scales and the classical behavior of macroscopic bodies has been debated since the inception of quantum theory. The fundamental difference is that while in quantum mechanics all configurations equivalent by symmetry have the same status, in classical physics one of them is singled out. This spontaneous symmetry breaking causes a macroscopic body under equilibrium conditions to have less symmetry than its microscopic building blocks.[1] Superconductors, antiferromagnets, liquid crystals, Bose-Einstein condensates, and crystals all exhibit spontaneously broken symmetries. The general idea is that when the number of microscopic quantum constituents N, which, depending on the system, corresponds to the number of Cooper pairs, particles, or spins, goes to infinity, the quantum system undergoes a phase transition into a state that violates the microscopic symmetries.[1,2] From a purely theoretical perspective, spontaneous symmetry breaking is thus related to a singularity of the thermodynamic limit. If this thermodynamic singularity is present, a symmetry-broken ground state exists. This observation can be formalized into an exact statement on the *existence* of a broken-symmetry state,[2,3] but it makes no assertion on whether or how it can evolve out of the symmetric state in a macroscopic body with N finite, nor on the dynamics of "quantum-classical" transitions. So the question remains how a continuous symmetry is broken *dynamically*.

We investigate this by considering a symmetry-breaking field slowly injected into an arbitrary large but finite system. If the symmetry-breaking process were fully adiabatic, the effect of the driving would correspond to subjecting the system to a quasistatic symmetry-breaking field. In this case the time scale at which quantum physics reduces to classical behavior and the correspondent symmetry-broken state is singled out becomes shorter and shorter as the size of the system grows. However, that the time evolution be adiabatic is not evident. The adiabatic theorem states that under slow enough external perturbations, there are no transitions between different energy levels. When the distance between energy levels is exponentially small, the adiabatic evolution is hampered and transitions between levels become unavoidable. Such dynamically induced excitations—"quantum defects"—can in principle strongly affect the symmetry-breaking process. Here we show that no matter how slowly a symmetry-breaking perturbation is driven, the adiabatic limit cannot be reached. Defect formation turns out to be so pervasive that it preempts an adiabatic symmetry breaking in macroscopic systems. The existence of this nonadiabatic regime is consistent with the breakdown of the adiabatic limit in low-dimensional gapless systems.[4]

The far-from-equilibrium time evolution caused by a symmetry-breaking field has remarkable consequences. We will show that in any large finite system the nonequilibrium state does not break the symmetry. However, it recursively collapses into the purely classical state: It breaks the symmetry at punctured times, resulting in a Dirac comb of symmetry-broken, classical states. This Dirac comb of quantum-classical transitions can be investigated in mesoscopic devices by supplying a proper dynamical symmetry-breaking perturbation. In ultracold atom systems, for instance, the necessary experimental prerequisites such as isolation from the environment, together with the possibility of real-time control of system parameters, are fulfilled.[5]

Even if *a priori* spontaneous symmetry breaking is an intractable problem involving a near infinity of interacting quantum degrees of freedom, there is a representative, integrable model that exhibits spontaneous symmetry breaking: the Lieb-Mattis model.[6–8] It is the effective collective Hamiltonian that underlies the breaking of the SU(2) spin rotation symmetry in generic Heisenberg models with short-range interactions. Very similar collective models underlie the breaking of other continuous symmetries as the gauge invariance in superconductors[9] or the translational symmetry in quantum crystals.[10] We therefore use the Lieb-Mattis antiferromagnet as a model system for dynamical symmetry breaking.

II. STATIC SYMMETRY BREAKING

The symmetry-breaking transition is manifest in the Lieb-Mattis model once a symmetry-breaking field H, in this case a staggered magnetic field, is introduced. Before turning to dynamical symmetry breaking, we first summarize a few essential features of the Lieb-Mattis Hamiltonian. The Hamiltonian is defined for spins 1/2 on a bipartite lattice with sublattices A and B, where $\mathbf{S}_{A,B}$ is the total spin on the A/B sublattice with z projection $S_{A/B}^z$:

$$\mathcal{H} = \frac{2|J|}{N}\mathbf{S}_A \cdot \mathbf{S}_B - H\big(S_A^z - S_B^z\big). \tag{1}$$

Every spin on sublattice A interacts with all spins on sublattice B and vice versa with an interaction strength $2|J|/N$ (which depends upon the number of sites N). Taking $H = 0$, the model can be solved by introducing the total spin operator $\mathbf{S} = \mathbf{S}_A + \mathbf{S}_B$. The eigenstates of the Hamiltonian are then $|S_A, S_B, S, M\rangle$, where S, M indicate the total spin and its z axis projection, whereas $S_{A,B}$ are the total sublattice spin quantum numbers. The ground state is symmetric and corresponds to an overall $S = 0$ singlet with $S_{A,B}$ maximally polarized and is characterized by zero staggered magnetization.

The $S \neq 0$ quantum numbers label a tower of states with energy scale $E_{\text{thin}} = J/N$, which is also referred to as the thin spectrum. It is *thin* because it contains states that are so sparse and of such low energy that their contribution to thermodynamic quantities vanish in the thermodynamic limit.[9,10] Nevertheless, when $N \to \infty$, the thin spectrum excitations collapse and form a degenerate continuum of states. Within this continuum, even an infinitesimally small symmetry-breaking perturbation H is enough to stabilize the fully ordered symmetry-broken ground state—the system is inferred to spontaneously break its symmetry. The finite symmetry-breaking field H couples the thin spectrum states so that the eigenstates $|n\rangle = \sum_S u_S^n |S\rangle$ of the Lieb-Mattis model become wave packets of total spin states. In the continuum limit, where N is large and $0 \ll S \ll N$, the corresponding low-energy effective Hamiltonian is[3]

$$\mathcal{H}_{\text{LM}} = \frac{HN}{4\hbar^2}\Pi^2 + \frac{J}{N}S^2, \tag{2}$$

where Π is the conjugate momentum of the total spin S. The eigenstates u_S^n are harmonic oscillator states of order n, with n odd in order to meet the boundary condition $S \geqslant 0$. In this case $E_{\text{thin}}^d = \sqrt{JH}$ represents the typical energy of the excitations labeled by n that now act as the thin spectrum in the symmetry-broken Hamiltonian. One can easily show the singular nature of the thermodynamic limit in the $n = 1$ ground state by calculating the expectation value of the order parameter[10]

$$\langle S_A^z - S_B^z \rangle \simeq \frac{N}{2}\int_1^\infty u_S^1 u_{S-1}^1 \, dS \simeq \frac{N}{2}e^{-\omega_S}, \tag{3}$$

where the dimensionless parameter $\omega_S = N^{-1}\sqrt{4J/H}$. When sending first $H \to 0$ and then $N \to \infty$, the singlet state appears as the ground state, which respects the spin rotational symmetry, i.e., $2\langle S_A^z - S_B^z \rangle \equiv 0$. Taking the limits in opposite order, one finds that the ground state corresponds to the fully polarized antiferromagnetic Néel state with a fully developed order parameter $2\langle S_A^z - S_B^z \rangle \equiv N$. Strictly speaking, Eq. (3) only allows truly infinite size systems to spontaneously select a direction for their sublattice magnetization. A large, but not infinitely large, system requires a finite symmetry-breaking staggered magnetic field to stabilize the symmetry-broken state over the exact spin singlet ground state. The strength of the required field obviously becomes increasingly weaker as the size of the antiferromagnet grows, and can be provided in practice by a magnetic impurity phase or by a second antiferromagnet.[11]

III. DYNAMIC SYMMETRY BREAKING: ADIABATIC-IMPULSE APPROACH

Let us now consider the dynamical case and turn on the symmetry-breaking field linearly in time $H(t) = \delta t$, with ramp rate δ. At initial time t_0 we start out with a field $H(t_0) = H_0$ (see the inset of Fig. 1) and the wave function of the system corresponding to this static ground state. We introduce H_0 in order to have a cutoff that guarantees the continuity of the wave-function basis. Later on we will consider the limit $H_0 \to 0$, which corresponds to an initial state that is a completely symmetric singlet. To capture the dynamics of the symmetry-breaking transition we first use the quantum Kibble-Zurek (KZ) theory.[12–14] The essence of the KZ theory of nonequilibrium phase transitions[15,16] is a splitting of the dynamics into a nearly critical impulse regime, where the system's state is effectively frozen and a quasiadiabatic regime far from the critical point. This splitting defines the so-called adiabatic-impulse approximation.[17] In particular, the critical impulse regime occurs whenever the characteristic relaxation time $\tau(t) = \hbar/E_{\text{thin}}^d(t)$ is much larger than the time scale t on which the Hamiltonian is changed. On the contrary, for $\tau(t) \ll t$, the system's state is able to adjust to the changing symmetry-breaking field, and the transitions among the dual thin spectrum excitations can be neglected. The crossover
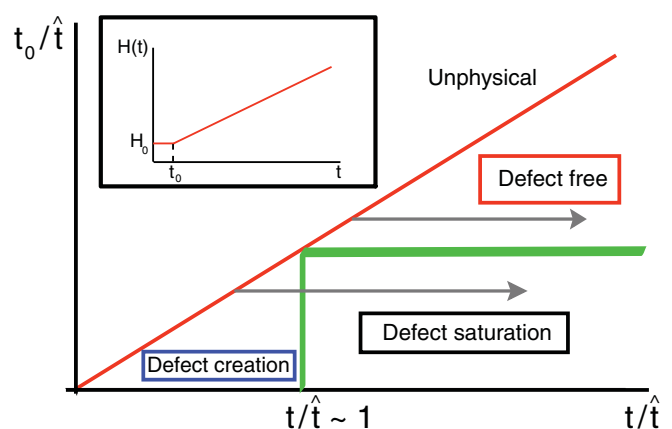

FIG. 1. (Color online) The three different regimes for the behavior of the density of defects in the t-t_0 plane. Times have been measured in units of the freeze-out time $\hat{t}$. The bold lines indicate the crossover among the different regimes, whereas the straight line limits the physical region with $t > t_0$. The gray arrows indicate different time trajectories. The inset shows the setup of the symmetry-breaking field.
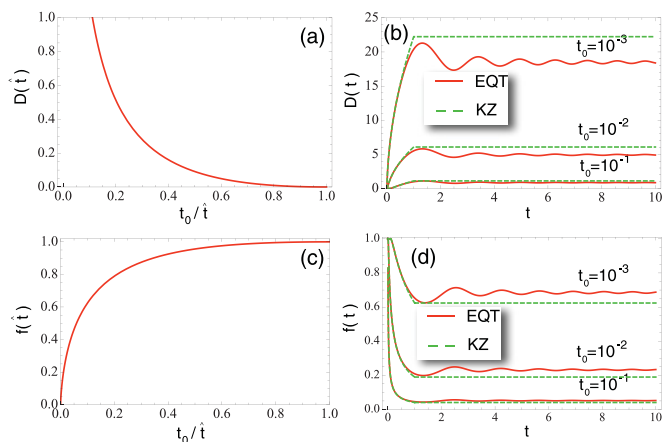
FIG. 2. (Color online) (a) Asymptotic value of the density of defects as a function of the initial time t_0 over freeze-out time $\hat{t}$ in the KZ theory. (b) Time evolution of the density of defects in the Lieb-Mattis model for different values of the initial time t_0. Times are measured in units of the freeze-out time $\hat{t}$. The continuous lines correspond to the exact quantum theory whereas the dashed lines indicate the time evolution in the KZ scheme. (c), (d) Same as (a), (b) for the fidelity of the ground-state wave function.

between the two regimes is determined by Zurek's equation[12] $\tau(\hat{t}) = \hat{t}$ and defines the freeze-out time

$$\hat{t} = \left[\frac{\hbar^2}{J\delta} \right]^{1/3}. \tag{4}$$

For an initial time $t_0 \gg \hat{t}$, the system's dynamics will thus be nearly adiabatic (cf. Fig. 1). Strictly speaking, in the true adiabatic limit ($t_0/\hat{t} \to \infty$), the probability of switching thin spectrum levels will be vanishingly small. This, in turn, implies that the fidelity of the snapshot ground-state wave function [cf. Figs. 2(c) and 2(d)]

$$f(t) = \left| \langle u_S^1(t) | \psi(t) \rangle \right|^2 \simeq 1,$$

where $\psi(t)$ is the actual ground-state wave function. We can also quantify the adiabaticity of the dynamical process by calculating the number of dynamically induced thin spectrum excitations, the density of "quantum defects"

$$\mathcal{D}(t) = \langle \psi(t) | \hat{n} - 1 | \psi(t) \rangle$$

vanishing in the truly adiabatic limit (cf. Fig. 2). The ramp rate of a nearly defect-free quench, however, is seen to be bounded by $\delta \ll \sqrt{H_0^3 J / \hbar}$ [cf. Eq. (4)]. Therefore, the limits $\delta \to 0$ and $H_0 \to 0$ do not commute. In other words, no matter how slowly one drives the symmetry-breaking field, if the initial symmetry breaking field H_0 is sufficiently small, the adiabatic limit can never be reached.

Besides just an adiabatic time evolution, the KZ analysis renders two nontrivial quantum dynamical regimes (cf. Fig. 1). First the evolution takes place in the impulse regime ($t_0 \ll t \ll \hat{t}$), where the initial state is effectively frozen and changes only by a trivial overall phase factor. The time evolution of both the density of defects and the fidelity of the snapshot ground-state wave function can be analyzed as follows: We expand the frozen initial ground state as a superposition of instantaneous thin spectrum eigenstates as

$$u_s^1(t_0) = \sum_n c_n u_s^n(t), \tag{5}$$

where the coefficients c_n are nonzero only for odd values of the quantum number n and depend on the ratio t_0/t as

$$c_n\left(\frac{t_0}{t} \right) = 4\sqrt{\frac{n!}{2^n}} \frac{1}{\left(\frac{n-1}{2} \right)!} \left(\frac{t}{t_0} \right)^{3/8} \frac{\left[1 - \sqrt{\frac{t}{t_0}} \right]^{(n-1)/2}}{\left[1 + \sqrt{\frac{t}{t_0}} \right]^{n/2+1}}. \tag{6}$$

For the fidelity of the snapshot ground-state wave function we then have

$$f(t) = 8\left(\frac{t}{t_0} \right)^{3/4} \frac{1}{\left[1 + \sqrt{\frac{t}{t_0}} \right]^3},$$

whose behavior is shown in Fig. 2(d) for different values of the initial time t_0. The density of dynamically generated defects instead grows continuously in time [cf. Fig. 2(b)] as

$$\mathcal{D}(t) = \frac{3}{4}\sqrt{\frac{t_0}{t}} \left[\sqrt{\frac{t}{t_0}} - 1 \right]^2. \tag{7}$$

This evolution lasts until $t > \hat{t}$. At the freeze-out time $\hat{t}$, defect formation stops and the defect density saturates [cf. Fig. 2(a)] to $\mathcal{D}(\hat{t}) \sim \frac{3}{4}\sqrt{\frac{\hat{t}}{t_0}}$. The defect density thus diverges for a small enough initial symmetry-breaking field H_0. Similarly, the fidelity saturates to $f(\hat{t}) \sim 8(t_0/\hat{t})^{3/4}$ [cf. Fig. 2(c)], which tends arbitrary close to 0 for a small enough initial time t_0. In this case the system actually reaches a state that is a superposition of a very large number of thin spectrum excitations. The symmetry-breaking process is thus accompanied by massive defect formation.

In the subsequent regime $t \gg \hat{t}$ no additional excitations are created. Since the evolution is considered to be adiabatic, we may write the time evolution of the wave function as

$$\psi_S(t) = \sum_n c_n\left(\frac{t_0}{\hat{t}} \right) u_S^n(t) e^{-i\Omega_n(t)},$$

where we have defined the dynamical phase

$$\Omega_n(t) = \hbar^{-1} \int_{\hat{t}}^t E_{\text{thin}}^d(t') \left(n + \frac{1}{2} \right) dt'$$

$$= \frac{2}{3}\left(n + \frac{1}{2} \right) [(t/\hat{t})^{3/2} - 1].$$

As the time increases, the various thin spectrum eigenstates all pick up a different dynamical phase leading to quantum interference. However, for $t_k = (1 + \frac{3k\pi}{2})^{2/3}\hat{t}$ with k integer, the interference is fully constructive and the wave function corresponds to the instantaneous ground state $u_S^1(tt_0/\hat{t})$, as can be straightforwardly verified. The system's state then corresponds precisely to the snapshot ground state of a symmetry-broken Lieb-Mattis model subject to a *renormalized* staggered magnetic field $H_R = H \times H_0/[\hbar^2\delta^2/(2J)]^{1/3}$. Thus when the initial symmetry-breaking field H_0 vanishes, the symmetric singlet state becomes fact at any recursion time and the SU(2) spin rotation symmetry is preserved.

IV. EXACT TIME EVOLUTION OF SYMMETRY BREAKING

A full description of the interference effects in a highly nonadiabatic state within the adiabatic-impulse method is, in practice, impossible. We can, however, explicitly monitor quantum phase interference effects by constructing the *exact* nonequilibrium wave function.

The dynamics of the time-dependent Hamiltonian Eqs. (2) indeed represents a simple example of generalized time-dependent harmonic oscillators whose exact quantum theory has been extensively studied in the literature.[18–30] Within the Feynman path integral approach, it can be shown[29] that the propagator has a spectral decomposition $\mathcal{G}(S_B, t_B | S_A, t_A) = \sum_n \Psi_{S_A}^{n\star}(t_A)\Psi_{S_B}^{n}(t_B)$ in terms of a complete set of wave functions of the form

$$\Psi_S^n(t) = \sqrt{\frac{1}{2^{n-1}n!}} \left[\frac{\mathrm{Re}[\omega(t)]}{\pi}\right]^{1/4} e^{-i(n+\frac{1}{2})\phi(t)}$$
$$\times H_n[\sqrt{\mathrm{Re}[\omega(t)]}S]e^{-\frac{S^2}{2}\omega(t)}, \tag{8}$$

where the quantum number n takes only odd values in order to meet the boundary condition $S \geqslant 0$, the H_n's are the usual Hermite polynomials, and $\mathrm{Re}(\omega) > 0$ to guarantee square integrability. The time-dependent dimensionless parameter ω can be explicitly obtained by identifying two linearly independent solutions to the classical Euler-Lagrange equation of motion

$$\ddot{S}_{1,2}^{\mathrm{cl}}(t)\frac{2\hbar^2}{\delta t N} - \dot{S}_{1,2}^{\mathrm{cl}}(t)\frac{2\hbar^2}{\delta N t^2} + \frac{2J}{N}S_{1,2}^{\mathrm{cl}}(t) \equiv 0. \tag{9}$$

Then the real and imaginary parts of the complex time-dependent dimensionless parameter ω read

$$\mathrm{Re}[\omega(t)] = \frac{2\hbar}{\delta N t}\frac{S_1^{\mathrm{cl}}(t)\dot{S}_2^{\mathrm{cl}}(t) - S_2^{\mathrm{cl}}(t)\dot{S}_1^{\mathrm{cl}}(t)}{S_1^{\mathrm{cl}}(t)^2 + S_1^{\mathrm{cl}}(t)^2},$$

$$\mathrm{Im}[\omega(t)] = -\frac{2\hbar}{\delta N t}\frac{S_1^{\mathrm{cl}}(t)\dot{S}_1^{\mathrm{cl}}(t) + S_2^{\mathrm{cl}}(t)\dot{S}_2^{\mathrm{cl}}(t)}{S_1^{\mathrm{cl}}(t)^2 + S_1^{\mathrm{cl}}(t)^2}, \tag{10}$$

whereas the quantal phase is determined by the differential equation

$$\dot{\phi}(t) = \mathrm{Re}[\omega(t)]\frac{\delta N t}{2\hbar}.$$

The classical equation of motion can be simplified by first changing the independent variable t to $z = 2/3(t/\hat{t})^{3/2}$ with $\hat{t}$ the freeze-out time. Under this transformation Eq. (9) is equivalent to

$$\ddot{S}^{\mathrm{cl}}(z) - \frac{1}{3z}\dot{S}^{\mathrm{cl}}(z) + S^{\mathrm{cl}}(z) = 0, \tag{11}$$

which can be explicitly solved in terms of Bessel functions

$$S^{\mathrm{cl}}(z) = C_1 z^{2/3} Y_{2/3}(z) + C_2 z^{2/3} \mathcal{J}_{2/3}(z), \tag{12}$$

with $C_{1,2}$ arbitrary real constants. The choice of these constants gives rise to different sets of wave functions.[29] Note that the propagator, however, does not depend upon this degree of freedom. To proceed further, we choose two classical solutions of the form Eq. (12) by taking $\{C_1, C_2\} = \{\lambda_1, 1\}, \{1, \lambda_2\}$. From Eq. (10) the real and imaginary parts of the dimensionless parameter ω can be recast as

$$\mathrm{Re}[\omega(t)] = \frac{2\hbar}{N\delta\hat{t}^2}\frac{3}{\pi}\left(\frac{3}{2}z\right)^{-\frac{4}{3}}\frac{1 - \lambda_1\lambda_2}{(1+\lambda_2^2)\mathcal{J}_{\frac{2}{3}}(z)^2 + 2(\lambda_1+\lambda_2)\mathcal{J}_{\frac{2}{3}}(z)Y_{\frac{2}{3}}(z) + (1+\lambda_1^2)Y_{\frac{2}{3}}(z)^2},$$

$$\mathrm{Im}[\omega(t)] = \frac{2\hbar}{N\delta\hat{t}^2}\left(\frac{3}{2}z\right)^{-\frac{1}{3}}\left\{\frac{(1+\lambda_2^2)\mathcal{J}_{-\frac{1}{3}}(z)\mathcal{J}_{\frac{2}{3}}(z) + (1+\lambda_1^2)Y_{-\frac{1}{3}}(z)Y_{\frac{2}{3}}(z)}{(1+\lambda_2^2)\mathcal{J}_{\frac{2}{3}}(z)^2 + 2(\lambda_1+\lambda_2)\mathcal{J}_{\frac{2}{3}}(z)Y_{\frac{2}{3}}(z) + (1+\lambda_1^2)Y_{\frac{2}{3}}(z)^2}\right.$$

$$\left. + \frac{(\lambda_1+\lambda_2)[\mathcal{J}_{\frac{1}{3}}(z)Y_{-\frac{1}{3}}(z) + \mathcal{J}_{-\frac{1}{3}(z)}Y_{\frac{2}{3}}(z)]}{(1+\lambda_2^2)\mathcal{J}_{\frac{2}{3}}(z)^2 + 2(\lambda_1+\lambda_2)\mathcal{J}_{\frac{2}{3}}(z)Y_{\frac{2}{3}}(z) + (1+\lambda_1^2)Y_{\frac{2}{3}}(z)^2}\right\}.$$

The free parameters $\lambda_{1,2}$ can be regarded as integration constants specified by the initial conditions. Indeed, they can be tuned in such a way that at the initial time $\mathrm{Re}[\omega(t_0)] \equiv \omega_S(t_0)$ and $\mathrm{Im}[\omega(t_0)] \equiv 0$. This, in turns, implies that the wave function will always remain an $n = 1$ state of the form Eq. (8) whose time dependence is completely adsorbed into the evolution of the dimensionless complex parameter ω. Having obtained the exact time evolution of the wave function, we can calculate the exact time dependence of the density of defects and the fidelity of the instantaneous ground-state wave function whose behavior is shown with the full lines in Figs. 2(b) and 2(d). The main features are well described by the foregoing adiabatic-impulse approximation and confirms the far-from-equilibrium dynamics for small enough initial symmetry-breaking fields H_0.

The resulting time dependence of the real part of ω for different values of t_0 is shown in Fig. 3(a). By decreasing the

initial time, it develops a series of sharp peaks whose position can be determined by the approximate form

$$\mathrm{Re}[\omega(t)] \sim \alpha\frac{1}{N}\sqrt{\frac{J}{\delta}}\frac{\sqrt{t_0}\hat{t}}{t^2}\mathcal{J}_{\frac{2}{3}}\left[\frac{2}{3}\left(\frac{t}{\hat{t}}\right)^{\frac{3}{2}}\right]^{-2}, \tag{13}$$

with the numerical constant $\alpha \sim 1.13$. In the $t_0 \to 0$ limit, it eventually leads to a Dirac comb structure [cf. Fig. 4(a)] with singularities at the zeros of the $\mathcal{J}_{2/3}$ Bessel function $t_k^R \simeq \hat{t}(\frac{3}{2}k\pi + \frac{13\pi}{8})^{\frac{2}{3}}$. The imaginary part of ω has a time dependence as in Fig. 3(c). As the initial time decreases, it approaches a characteristic tangent-like behavior [cf. Fig. 4(b)]

$$\mathrm{Im}[\omega(t)] = \frac{1}{N}\sqrt{\frac{J}{\delta}}\frac{1}{\sqrt{t}}\frac{\mathcal{J}_{-\frac{1}{3}}\left[\frac{2}{3}\left(\frac{t}{\hat{t}}\right)^{\frac{3}{2}}\right]}{\mathcal{J}_{\frac{2}{3}}\left[\frac{2}{3}\left(\frac{t}{\hat{t}}\right)^{\frac{3}{2}}\right]}, \tag{14}$$
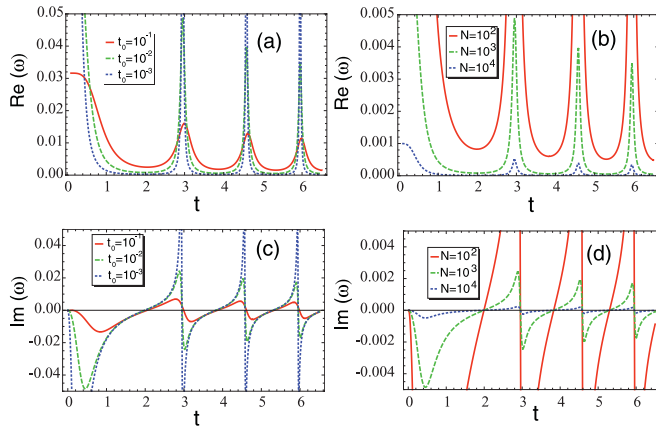
FIG. 3. (Color online) (a) Time dependence of the real part of the dimensionless parameter ω for different values of the initial time t_0 for $N = 10^2$ spins and a freeze-out time $\hat{t} = 1$. All times are measured in units of $4J/\delta$. (b) Same for a fixed initial time $t_0 = 10^{-2}$ and different values of the number of sites N. (c), (d) Same as (a), (b) for the imaginary part of the dimensionless parameter ω.

with singularities appearing precisely at the Dirac deltas of $\mathrm{Re}(\omega)$ and zeros at the punctured instants $t_k^I \simeq \hat{t}(\frac{3}{2}k\pi + \frac{7\pi}{8})^{\frac{2}{3}}$. The limiting behavior of ω is universal since it scales with N^{-1} as the number of sites is varied [cf. Figs. 3(b) and 3(d)]. As a result, any large but finite system displays the fully symmetric singlet state and the classical symmetry-broken ground state at the punctured times t_k^R and t_k^I, respectively. In between, the system's state has an intermediate structure characterized by a vanishing real part and a finite imaginary part that preserves the SU(2) spin rotation symmetry, as we show below.

We can in fact obtain the exact evolution of the order parameter by considering that the expectation value of the staggered magnetization is given by

$$\langle S_A^z - S_B^z \rangle = \sum_{S,S'} \Psi_S^1 \Psi_{S'}^{1\star} \langle S' | S_A^z - S_B^z | S \rangle. \quad (15)$$
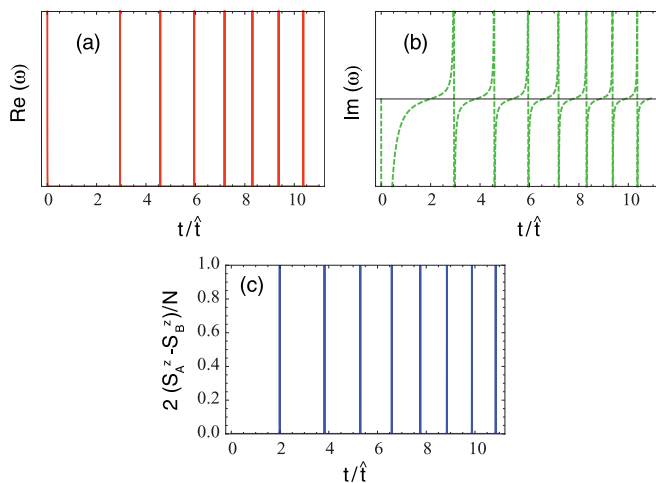

FIG. 4. (Color online) Asymptotic behavior of the real (a) and the imaginary (b) part of the dimensionless parameter ω in the limit $t_0 \to 0$. (c) Asymptotic behavior of the order parameter as a function of time measured in units of the freeze-out time $\hat{t}$.

The matrix elements are nonzero for consecutive thin spectrum levels alone[10] $\langle S' | S_A^z - S_B^z | S \rangle = f_{S'+1} \delta_{S',S-1} + f_{S'} \delta_{S',S+1}$. In the continuum limit where N is large and $1 \ll S \ll N$, one has[10] $f_S \sim N/4$ and consequently the expectation value of the order parameter is determined by the evolution of the complex dimensionless parameter ω via

$$\frac{2\langle S_A^z - S_B^z \rangle}{N} = \frac{4\,\mathrm{Re}(\omega)^{3/2}}{\sqrt{\pi}} \int_1^\infty dS\, S(S-1)$$
$$\times \cos\left[\frac{\mathrm{Im}(\omega)}{2}(2S-1)\right] e^{-\frac{\mathrm{Re}(\omega)}{2}[S^2+(S-1)^2]}.$$

A vanishing real part of ω accompanied by a finite value $\mathrm{Im}(\omega)$ guarantees that the spin rotation symmetry is unbroken. A Dirac comb structure for the time evolution of the order parameter is the result:

$$2\langle S_A^z - S_B^z \rangle = N \sum_{k \geqslant 0} \delta_{t,t_k^I}, \quad (16)$$

as is shown in Fig. 4(c).

V. CONCLUSIONS

The exact time development reveals that when a symmetric Lieb-Mattis system is subject to a symmetry-breaking field, a nonequilibrium state forms that is intermediate between a pure quantum symmetric and a pure classical state. It is a vast superposition of thin spectrum excitations with complex amplitudes. This state *does not* break the spin rotation symmetry, as direct computation of the order parameter demonstrates. As time evolves, this nonequilibrium state develops smoothly, until at a certain moment the system's state corresponds *precisely* to a fully developed classical ground state. This classical state forms at punctured times where the imaginary part of ω vanishes. At any other instant, the spin rotation symmetry is restored. This is in agreement with the adiabatic-impulse analysis which does not allow symmetry breaking of a symmetric state when quantum phase interference effects are neglected.

As a result, the time evolution of the order parameter is characterized by a comb structure [cf. Fig. 4(c)], which corresponds to the periodic emergence of the symmetry-broken states at punctured times. These instants are related to the freeze-out time alone, indicating the nonequilibrium nature of this dynamical symmetry-breaking phenomenon. The freeze-out time can be experimentally tuned by changing the ramp rate of the symmetry-breaking field, and a quantum-classical transition can be induced in individual mesoscopic quantum objects by supplying a proper dynamical symmetry-breaking perturbation. In the case of an infinitely sudden quench ($\delta \to \infty$), the freeze-out time vanishes and the punctured times of symmetry-broken classical states collapse onto each other. In the contrary, asymptotically adiabatic limit ($\delta \to 0$), the first punctured time of the symmetry-broken state diverges: The system never breaks its symmetry.

In the dynamical realm the quantum-classical symmetry-breaking transition is thus characterized by far-from-equilibrium processes. The exact continuum theory shows that no matter how slowly the symmetry-breaking process is

driven, defect formation prevents an adiabatic time evolution. In a closed system, therefore, a stable symmetry-broken state

cannot evolve out of a symmetric quantum state—neither spontaneously nor by driving it.

[1] P. W. Anderson, Science **177**, 393 (1972).

[2] P. W. Anderson, Phys. Rev. **86**, 694 (1952).

[3] J. van Wezel, J. van den Brink, and J. Zaanen, Phys. Rev. Lett. **94**, 230401 (2005).

[4] A. Polkovnikov and V. Gritsev, Nat. Phys. **4**, 477 (2008).

[5] I. Bloch, J. Dalibard, and W. Zwerger, Rev. Mod. Phys. **80**, 885 (2008).

[6] E. Lieb and D. Mattis, J. Math. Phys. **3**, 749 (1962).

[7] C. Kaiser and I. Peschel, J. Phys. A **22**, 4257 (1989).

[8] T. A. Kaplan and W. von der Linden, and P. Horsch, Phys. Rev. B **42**, 4663 (1990).

[9] J. van Wezel and J. van den Brink, Phys. Rev. B **77**, 064523 (2008).

[10] J. van Wezel, J. Zaanen, and J. van den Brink, Phys. Rev. B **74**, 094430 (2006).

[11] J. van Wezel, Phys. Rev. B **78**, 054301 (2008).

[12] W. H. Zurek, U. Dorner, and P. Zoller, Phys. Rev. Lett. **95**, 105701 (2005).

[13] A. Polkovnikov, Phys. Rev. B **72**, 161201 (2005).

[14] B. Damski, Phys. Rev. Lett. **95**, 035701 (2005).

[15] T. W. B. Kibble, Phys. Rep. **67**, 183 (1980).

[16] W. H. Zurek, Nature (London) **317**, 505 (1985).

[17] B. Damski and W. H. Zurek, Phys. Rev. A **73**, 063405 (2006).

[18] D. C. Khandekar and S. V. Lawande, Phys. Rep. **137**, 115 (1986).

[19] D. C. Khandekar and S. V. Lawande, J. Math. Phys. **20**, 1870 (1979).

[20] R. Colegrave and M. Abdalla, J. Phys. A **14**, 2269 (1981).

[21] R. Colegrave and M. Abdalla, J. Phys. A **15**, 1549 (1982).

[22] R. Colegrave and M. Abdalla, J. Phys. A **16**, 3805 (1983).

[23] M. S. Abdalla and R. K. Colegrave, Phys. Rev. A **32**, 1958 (1985).

[24] M. S. Abdalla, Phys. Rev. A **34**, 4598 (1986).

[25] M. S. Abdalla, Phys. Rev. A **33**, 2870 (1986).

[26] G. J. Papadopoulos, J. Phys. A **7**, 209 (1974).

[27] K. H. Yeon, K. K. Lee, C. I. Um, T. F. George, and L. N. Pandey, Phys. Rev. A **48**, 2716 (1993).

[28] A. Lopes de Lima, A. Rosas, and I. A. Pedrosa, Ann. Phys. **323**, 2253 (2008).

[29] D.-Y. Song, Phys. Rev. A **59**, 2616 (1999).

[30] D.-Y. Song, Phys. Rev. Lett. **85**, 1141 (2000).